

## Removal of Acid Blue 25 Dye from Wastewater using Rambutan (*Nephelium lappaceum* Linn.) Seed as an Efficient Natural Biosorbent

Sivarama Krishna Lakkaboyana<sup>1,2,5\*</sup>, Soontarapa Khantong<sup>1,2\*</sup>, Mohammad Alamgir Kabir<sup>3,5</sup>, Yuzir Ali<sup>4</sup>, Wan Zuhairi Wan Yaacob<sup>5</sup>

<sup>1</sup>Department of Chemical Technology, Chulalongkorn University, Bangkok, Thailand, <sup>2</sup>Center of Excellence on Petrochemical and Materials Technology, Chulalongkorn University, Pathumwan, Bangkok, Thailand, <sup>3</sup>Geological Survey of Bangladesh, Segunbagicha, Dhaka, Bangladesh, <sup>4</sup>Department of Environmental Engineering and Green Technology, Malaysia-Japan International Institute of Technology, Universiti Teknologi Malaysia, Jalan Sultan Yahya Petra, Kuala Lumpur, <sup>5</sup>Geology Programme, Faculty of Science and Technology, School of Environmental Sciences and Natural Resources, Universiti Kebangsaan Malaysia, Bangi, Selangor, Malaysia.

### ABSTRACT

The potential of Rambutan seeds (RSs) for biosorption of acid blue 25 (AB25) from aqueous solutions was investigated in batch systems in terms of kinetics and equilibrium. Experimental data showed that the biosorption capacity of RS was dependent on operating variables such as solution pH, initial AB25 dye concentration, and contact time. The maximum biosorption has occurred at pH 2 (87.06%). Significant enhancement of AB25 biosorption was observed by increasing initial dye concentration. Adsorption kinetic data were fitted using the pseudo-first-order, pseudo-second-order (PSO), and intraparticle diffusion model. The biosorption kinetics for the AB25 dye onto RS was best described by PSO kinetic model. Langmuir model exhibited the best fit to experimental data. According to this adsorption isotherm model, the maximum AB25 biosorption capacity of RS is 35.58 mg/g. The low  $R_L$  values (0.1357–0.0497) also confirmed that RS biomass is favorable for biosorption of AB25. The results reveal that adsorption is proceed with the chemisorption process. These results indicate that RS can be used as an effective and environmentally friendly biosorbent to remove AB25 from wastewater.

**Key words:** Rambutan seed, Biosorption, Kinetic, Isotherms, Acid blue 25, Wastewater.

### 1. INTRODUCTION

Nowadays, different types of technologies are used for the treatment of dye wastewater such as adsorption, advanced oxidation process, biological treatment, coagulation-flotation, electrochemical process, flotation, filtration, ion-exchange membrane, super filter film, oxidation, and electrolysis [1-4]. Most of these methods for the treatment of dye wastewater have not been widely applied at large scale, because of the high cost and disposal problems. Among these methods, the adsorption process is one of the effective techniques that have been successfully employed for dye removal from wastewater. Activated carbon is the popular adsorbent material most commonly applied for adsorption process of dyes. However, because of its high price and hard regeneration the wide applications of activated carbon were limited [5-7]. Recently, the researchers are focused on the development of low-cost adsorbents for the application of adsorption technique for wastewater treatment. Because of adsorption method having much more advantages, such as the low cost, availability, profitability, ease of operation, and efficiency, in comparison with methods, especially from economic and environmental points of view and also cannot produce any harmful substances in this process. However, the use of activated carbon as an adsorbent is disadvantageous because it is relatively expensive. For this reason, a number of nonconventional low-cost materials have recently been attempted and included as alternative adsorbent to activated carbon for the removal of dyes from wastewater. Especially, agriculture by-products and waste materials from fruits and vegetables are considered as low-cost adsorbents since it is abundant

in nature, inexpensive, requires little processing, and is an effective material [8,9]. Recently, different varieties of materials have been used as low-cost adsorbents, those are mainly fruit seeds, agricultural by-products, and vegetable waste such as Jujuba seeds [1,2,7], papaya seeds [10], cashew nut shell [11], *Luffa cylindrica* cellulosic fiber [12], palm kernel coat [13], *Thuja orientalis* cone powder [14], wheat straw [5,15], *Cicer arietinum* Linn. fruit shell [16], and some reviews on agricultural waste [9,17,18].

This work aims to evaluate the potential of RS as a novel biosorbent for dye removal, and removal of organic pollutant from aqueous solution is very interesting from the economic point of view since it is an agricultural residue that is available at low cost. In this context, the aim of the present study was to investigate the potential application of Rambutan seeds (RSs) as a biosorbent for the removal of textile dye AB25 from wastewater. Kinetics, equilibrium, and mechanism studies were carried out to elucidate the biosorption process of AB25 dye onto RSs.

#### \*Corresponding author:

E-mail: svurams@gmail.com/khantong.s@chula.ac.th

ISSN NO: 2320-0898 (p); 2320-0928 (e)

DOI: 10.22607/IJACS.2018.603003

Received: 28<sup>th</sup> March 2018;

Revised: 02<sup>nd</sup> May 2018;

Accepted: 02<sup>nd</sup> June 2018

## 2. MATERIALS AND METHODS

### 2.1. Biomaterial Preparation

Rambutan (*Nephelium lappaceum* Linn.) fruits were collected at the local market, in Bangi, Selangor, Malaysia. We are consuming the pulp and separate the seed from fruits. After taking out the pulp of the fruits, the RSs were thoroughly washed with tap water to remove the pulp left, if any and were sun dried. The dried seeds were pulverized into a fine powder in a mechanical grinder and sieved to desire mesh sizes standard sieves. The sieved biomaterial was stored in an airtight plastic container, label as RS, until used for the experiments. RS biosorbent was used in the AB25 biosorption experiments performed in this work. The Rambutan fruit belongs to the family of *Sapindaceae* and its botanical name is *N. lappaceum* Linn.

### 2.2. Adsorbate

Acid blue 25 (AB25) dye was used in this study; it is purchased from Sigma-Aldrich, Selangor, Malaysia. Its C.I. No. 62055 and its chemical formula= $C_{20}H_{13}N_2NaO_5S$  (FW=416.38 g) and  $\lambda_{max}=610$  nm. The chemical was used without any further purification. Stock solution of 1000 mg/l was prepared by dissolving 1 g accurate quantity of the AB25 in distilled water. The experimental solution was obtained by diluting the stock solution to the designed initial AB25 concentration.

### 2.3. Batch Biosorption Studies and Analytical Method

In batch biosorption kinetics, 25 ml of solutions of AB25 of varying concentrations (25–75 mg/l) in 50 mL centrifuge tubes a fixed mass of the biosorbent was added and the content was shaken on a rotatory shaker for 5–120 min. The solution was centrifuged and the concentration of residual AB25 was determined spectrophotometrically at 610 nm. For kinetic measurements, the experiments were performed using a fixed biosorbent dose with varying contact times at different AB25 dye concentrations. The effect of pH on AB25 dye removal was studied over a pH range of 2–12. The pH was adjusted by adding a few drops of 1.0 N NaOH or 1.0 N HCl. In this study, 25 mL of a fixed initial concentration of AB25 at different pH was agitated with 50 mg of RS biosorbent for 120 min. The effect of RS dose on the amount of AB25 adsorbed is obtained by taking different amounts of RS (10–100 mg) and agitated for 120 min with 50 mg/l solution of AB25 at original pH of AB25.

The samples were withdrawn from the shaker at predetermined time intervals, and the AB25 solution was separated from the biosorbent by centrifugation at 10,000 rpm for 10 min. The absorbance of supernatant solution was measured, from which the amount of AB25 adsorbed was calculated.

The amount of biosorption at time  $t$ ,  $q_t$  (mg/g), was calculated using the following equation:

$$qt = [(C_0 - C_t)V] / W \quad (1)$$

Where,  $C_0$  and  $C_t$  (mg/l) are the liquid phase concentrations of AB25 at initial and at any time  $t$ , respectively.  $V$  is the volume of the solution (L) and  $W$  is the mass of dry biosorbent used (g).

The AB25 removal percentage can be calculated as follows:

$$\text{Removal percentage} = [(C_0 - C_e) / C_0] * 100 \quad (2)$$

Where,  $C_e$  is the equilibrium concentration in solution (mg/l).

### 2.4. Determining the Point of Zero Charge (pHpzc)

The  $pH_{pzc}$  of the RS biomass was determined by the solid addition method [1,2,19]. In this experiment, 0.05 g of RS biosorbent was added to 25 ml 0.1 M potassium nitrate ( $KNO_3$ ) solution. The pH

values were adjusted to between 2 and 12 at two intervals, using the 1.0 M hydrochloric acid (HCl) and 1.0 M sodium hydroxide (NaOH). The solution with the RS biosorbent was equilibrated for 24 h. After 24 h of shaking, all conical flasks were withdrawn from the shaker and allowed to equilibrate for 0.5 h. Afterward, the final pH of the solutions was recorded. The intersection point of the curve  $\Delta pH$  ( $pH_i - pH_f$ ) versus  $pH_i$  is considered as the amount of point zero charge.

## 3. RESULTS AND DISCUSSION

### 3.1. RS biomass Characterization

The infrared spectra in the range of 4000–400  $cm^{-1}$  were recorded for the RS biomass and AB25 dye loaded RS biomass. Fourier transform-infrared (FTIR) analysis was conducted to determine the presence of the functional groups and their possible interactions with AB25 dye. The RS biomass FTIR spectrum is shown in Figure 1. The peaks observed at 3991  $cm^{-1}$  assigned as bounded hydroxyl O-H group. The peaks are observed at 3467 and 3431  $cm^{-1}$  assigned as N-H stretching vibration and C=O bond in amide group. The band at 1744  $cm^{-1}$  to 1736  $cm^{-1}$  assigned as C-O bond in carboxylic acid and C=O bond in carboxylates. The band at 2851 and 2917  $cm^{-1}$  assigned as O-H in alcoholic group. Remaining other peaks 2225, 2165, 2344, and 2360  $cm^{-1}$  indicate the presence of C-H asymmetric and symmetric stretching.

The RS is characterized by the bands: The broadband in the 3467  $cm^{-1}$  region is ascribed to N-H stretching vibration, C-O band occurs at 11,644  $cm^{-1}$  assigned as associated with the amide group, and the band at 3271  $cm^{-1}$  and 3295  $cm^{-1}$  assigned as alcoholic O-H group stretching vibration. The band at 1744  $cm^{-1}$ –1736  $cm^{-1}$  assigned as -COO carbonyl peak. The bands between 2851  $cm^{-1}$  and 2917  $cm^{-1}$  assigned as OH band of carboxylic group. Figure 1 confirmed the presence mainly of carboxyl, hydroxyl, and amide/amines functional groups on the biosorbent surface. These groups are led to bind with the dye  $-SO_3$  and  $NH_2$  group; these interactions are shown in Figure 2.

The morphological characteristics of the biosorbent were studied by SEM analysis (Figures 3 and 4). Figures 3 and 4 are shows the SEM micrographs of RS samples before and after AB25 dye biosorption. It is clear that RS has considerable numbers of heterogeneous pores where there is a good possibility for dye to be trapped and adsorbed. The surface of dye-loaded adsorbent, however, clearly shows that the surface of RS is covered with dye molecules.

### 3.2. Effect of Biosorbent Mass

The effect of biosorbent (RS) mass on the removal of AB25 from the wastewater is shown in Figure 5. When the biosorbent mass was increased from 0.01 to 0.1 g, an increase in the AB25 removal percentage also increased up to 0.05 g afterward gradually decreased up to 0.1 g. This behavior could be explained considering that with biosorbent dosage increases it occurs an increase on the surface, consequently, more active sites are available to bind dye from aqueous phase [2]. At masses over 0.05 g, the amount of AB25 biosorbed decreases gradually due to the aggregation of particles of biosorbent in the solution, consequently, a decrease in the surface for dye uptake occurs. Similar results regarding the effect of biosorbent dose on dye biosorption capacity have been observed and discussed in the literature [20–22]. For this reason, the biosorbent mass 0.05 g was chosen for the kinetics experiments.

### 3.3. Effect of Initial pH

Previous reports in the literature have shown that solution pH is an important parameter affecting the biosorption process. Due to the protonation of the functional groups on the biosorbent surface and the chemistry of dye molecules are strongly affected by the pH of the

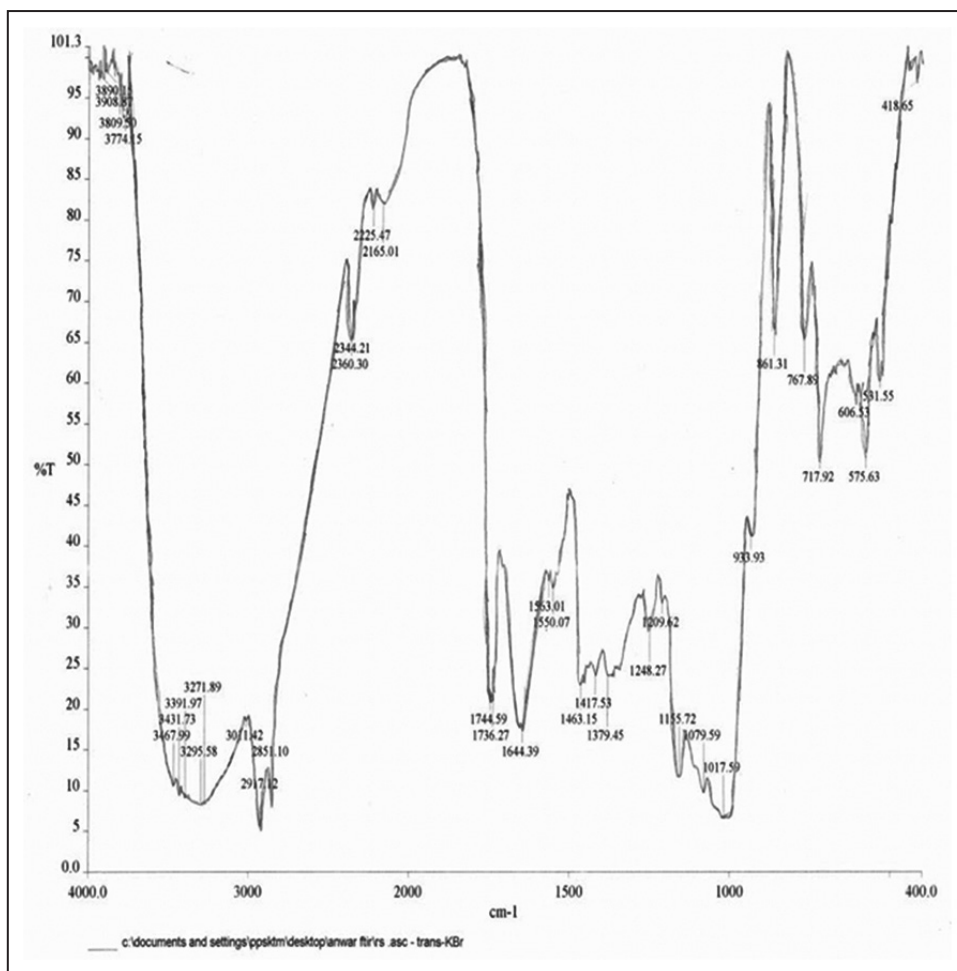


Figure 1: Fourier transform-infrared spectra of Rambutan seeds

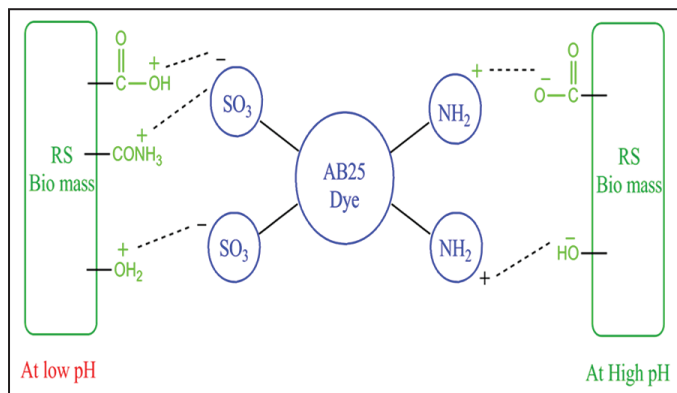
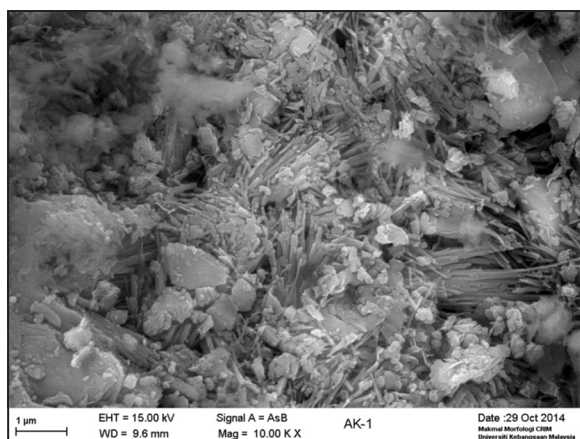


Figure 2: Adsorption mechanism

solution. In this experiment, the effect of initial solution pH on the biosorption of AB25 was evaluated over a range of pH values from 2 to 12 using initial AB25 concentration of 50 mg/l, at temperature of 30°C, using 50 mg of biosorbent (Figure 6). From Figure 5, the maximum removal efficiency is achieved at pH 2. It can be observed that the process of biosorption is highly dependent on the pH value of the solution. The removal efficiencies of AB25 dye decrease, with an increase in the value of the pH of the solution. The uptake of AB25 removal percentage was decreased significantly from 87.06% to 29.09% as the pH solutions increased from 2 to 12. This result could be interpreted as an electrostatic interaction between the surface of the biosorbent, positively charged, and the anionic AB25 dye [1]. At lower

pH values, a possible protonation of carboxylate group (COOH) and alcohols (OH), amine and amide (NH<sub>2</sub>) at the surface RS can occur, resulting in more attraction force between the anionic AB25 dye and protonated COOH, OH, and NH<sub>2</sub> groups. Thus, at pH 2, the removal efficiency of AB25 is very high (87.06%). The pH values ranging from 6 to 12, negative carboxylic (COO<sup>-</sup>) and alcohol (OH) groups are an increase with increasing the pH, due to these changes biosorption was decreased. Because of biosorbent having the more negatively charged species and AB25 dye also having negative SO<sub>3</sub><sup>-</sup> species, due to the high electrostatic repulsion between the negatively charged surface of RS and AB25 (Figure 2). This condition may be decreasing the AB25 removal percentage from aqueous solution.

The point of zero charge value (pH<sub>PZC</sub> 6) of the biosorbent confirms this behavior (Figure 7). At pH < 6, the RS surface is positively charged, hindering the electrostatic attraction of AB25, an anionic dye. At pH > 6, the AB25 biosorption is hindered because the surface of biosorbent is negatively charged and dye molecule also having negative charge. Figure 6 shows that the best pH values for AB25 biosorption on RS are pH 2. Similar results were reported for the AB25 removal using IJSP [1] and removal of Victazol orange 3R by mangifera indica seed, removal of Evans blue and Vilmafix red (RR-2B) dyes by aquatic stalks [23], durian peel toward the acidic dye [24], removal of acid blue 062 by calcined colemanite ore waste [25], and acid 183 and acid green 25 onto shell of bittim [26], diatomite [27], AB25 onto spent brewery grains (SBGs) [28], AB25 onto waste tea activated carbon [29], and AB25 onto natural sepiolite [30]. Therefore, pH 2 was selected for further biosorption experiments.



**Figure 3:** Scanning electron microscopic photograph of Rambutan seeds alone

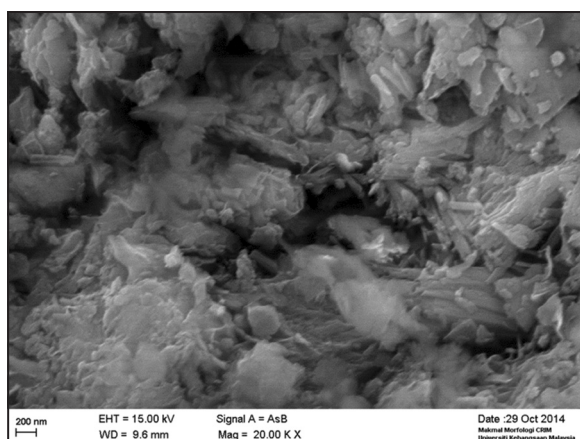


**Figure 4:** Scanning electron microscopic photograph of acid blue 25 loaded Rambutan seeds

### 3.4. Dye removal Mechanism

AB25 is anionic dye; these anionic molecules increased the biosorption in an acidic medium. Figure 2 shows, at lower pH, available of excessive in  $H^+$  ion in the solution, these  $H^+$  ions interact with anionic AB25, so biosorption rate is higher at pH 2. Due to these reasons, the molecules of dye anions bind at the sorption sites at the surface of biosorbent. Thus, enhance the capability of the binding activity between dye anions and sorbent surface through electrostatic forces of attraction. Meanwhile, the removal of dye is low at high pH due to the excess of hydroxide ions,  $OH^-$  competing with the molecules of dye anions to bind at the sorption sites at the surface of biosorbent. At higher pH, between pH 7 and 11, also adsorption occurred due to interaction of amine's groups of AB25 with carboxyl groups of RS biomass. It is proved in pH effect. A similar trend was observed for adsorption of AB25 onto IJSP [1], diatomite [27], SBGs [28], waste tea activated carbon [29], and natural sepiolite [30].

## 4. ADSORPTION ISOTHERM MODELS

Adsorption equilibrium provides fundamental physiochemical data for evaluating the applicability of the adsorption process as a unit operation. The two most commonly used equilibrium relations are Langmuir and Freundlich isotherm equations.

### 4.1. Langmuir Isotherm Model

The Langmuir isotherm model anticipates the existence of monolayer coverage of the sorbate molecules over a homogeneous sorbent surface,

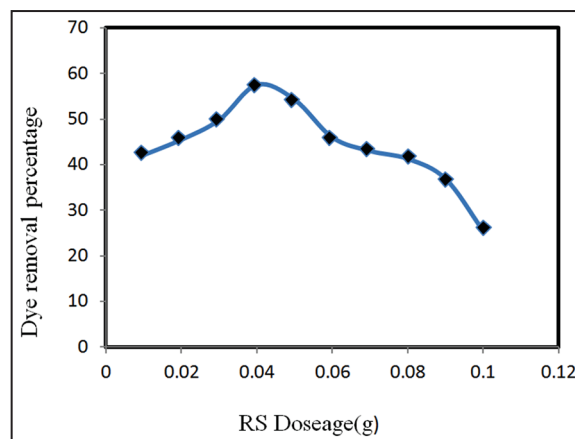


**Figure 5:** Effect of biosorbent dose on the biosorption of acid blue 25 on to Rambutan seeds

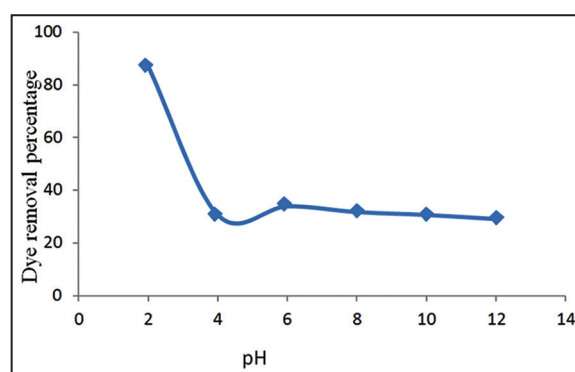


**Figure 6:** Effect of pH on equilibrium uptake of acid blue 25

and there is no important interaction among the sorbed species. The Langmuir model also assumes that the sorbent surface contains only one type of binding site so the energy of sorption is constant. The Langmuir isotherm model expressed by the following equation [1]:

$$q_e = bQ_{max}C_e / (1 + bC_e) \quad (3)$$

Where,  $q_e$  (mg/g) is the amount of the dye biosorbed per unit mass of biosorbent,  $C_e$  (mg/l) is the equilibrium dye concentration in the solution,  $Q_{max}$  (mg/g) is the Langmuir maximum monolayer sorption capacity, and  $b$  (L/mg) is the constant.

The Langmuir model in linear form can be written as Eq. 4:

$$\text{Langmuir isotherm model: } (C_e/q_e) = (1/Q_{max}b) + (C_e/Q_{max}) \quad (4)$$

The linear plot of  $C_e$  versus  $C_e/q_e$  shows that sorption obeys the Langmuir model and the constants  $Q_{max}$  and  $b$  are evaluated from slope and intercept of the linear plot, respectively.

The essential characteristics of Langmuir isotherm can be described by means of " $R_L$ " a dimensionless constant referred to as separation factor or equilibrium parameter.  $R_L$  can be calculated using the following Eq. 5.

$$\text{Separation factor: } R_L = 1 / (1 + K_L C_0) \quad (5)$$

Where,  $C_0$  is the initial dye concentration, and  $K_L$  is the Langmuir constant. The values of  $R_L$  indicate the type of isotherm to be favorable ( $0 < R_L < 1$ ), unfavorable ( $R_L > 1$ ), irreversible ( $R_L = 0$ ), or linear ( $R_L = 1$ ). By processing the above equation,  $R_L$  values for investigated RS-AB25 system are found to be 0.1357–0.0497. From the values of  $R_L$ , it is confirmed that RS biomass is favorable for biosorption of AB25 dyes from wastewater.

The experimental equilibrium data of AB25 were compared with the theoretical equilibrium data obtained from Langmuir isotherm model. The biosorption data were analyzed using the linear form of Langmuir isotherm (Eq. 4). The values of  $Q_{max}$  and  $b$  obtained from the slope and intercept of the linear plot of  $C_e/q_e$  versus  $C_e$ . The adsorption monolayer capacity is 35.58 mg/g, with correlation coefficient ( $R^2$ ) of 0.9961. The  $R_L$  values ranged from 0.1357 to 0.0497 between 25 and 75 mg/g of initial AB25 concentration. From the results, the biosorption of AB25 onto RS biomass was well fitted with the Langmuir isotherm model.

4.2. Freundlich Isotherm Model

The Freundlich isotherm model assumes a heterogeneous sorption surface with sites that have different energies of sorption and provides no information on the monolayer adsorption capacity [26]. The Freundlich model can be written as Eq. 6:

$$q_e = K_f C^{1/n} \tag{6}$$

Where,  $K_f$  is a constant related to sorption capacity (mg/g) and  $1/n$  is an empirical parameter related to sorption intensity. The value of  $n$  varies with the heterogeneity of sorbent and gives an idea for the favorability of sorption process. The value of  $n$  should be  $<10$  and higher than unity for favorable sorption conditions. The Freundlich model in linear form can be written as Eq. 7:

Freundlich isotherm model:  $\log q_e = \log K_f + (1/n) \log C_0$  (7)

The experimental equilibrium data were also compared with the theoretical equilibrium data obtained from Freundlich isotherm model. The values of Freundlich constants,  $K_f$  and  $1/n$ , were obtained according to the linear form of the Freundlich isotherm (Eq. 7) and found to be 12.13 and 3.57 mg/g, respectively, with correlation coefficient ( $R^2$ ) of 0.9673. The Freundlich constant  $1/n$  was smaller than unity indicated that the biosorption process was favorable under studied conditions. It is clear that the biosorption pattern of AB25 onto RS was well fitted with both the Langmuir and Freundlich isotherm models. This may be due to both homogeneous and heterogeneous distribution of active sites on the surface of the RS.

5. BIOSORPTION KINETICS

To predict the mechanism of the present biosorption process and evaluate the performance of the biosorbent for dye removal, three well-known kinetic models were used to fit the experimental data; pseudo-first-order (PFO), pseudo-second-order (PSO), and intraparticle diffusion models [2,19].

5.1. PFO Model

The PFO kinetic model was described by Lagergren:

PFO model:  $\log (q_e - q_t) = \log q_e - (k_1/2.303) t$  (8)

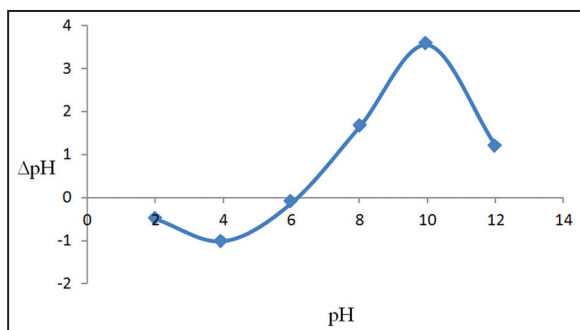


Figure 7: Point zero charge (pHPZC) of Rambutan seeds

Where,  $q_e$  (mg/g) and  $q_t$  (mg/g) are the amounts of the dye, biosorbed on the biosorbate at equilibrium and at any time  $t$ , respectively; and  $k_1$  (1/min) is the rate constant of the first-order model.

A straight line of  $\log (q_e - q_t)$  versus  $t$  suggests the applicability of this kinetic model and  $q_e$  and  $k_1$  can be determined from the intercept and slope of the plot, respectively. It is important to notice that the experimental  $q_e$  must be known for the application of this model. Table 1 summarizes the PFO constants,  $q_e$  and  $k_1$ , along with the corresponding correlation coefficients for investigated initial AB25 concentrations. The correlation coefficients were found in the range from 0.6338 to 0.9978, which were relatively low. There was a deviation from the straight line of  $\log (q_e - q_t)$  versus  $t$  (Figure not shown) after the first 20 min for all investigated initial dye concentrations, indicating that the PFO model was only applicable for the first 20 min of biosorption. These observations suggested that the PFO model is not suitable for modeling the biosorption of AB25 onto RS.

5.2. PSO Model

The PSO model based on the assumption that the rate-limiting step is chemical sorption or chemisorption involving valance forces through sharing/exchange of electrons between sorbent and sorbate as covalent forces.

PSO model:  $t/q_t = (1/k_2 q_e^2) + (1/q_e) t$  (9)

Where,  $k_2$  (g/mg/min) is the rate constant of the second-order equation,  $q_e$  (mg/g) is the maximum biosorption capacity, and  $q_t$  (mg/g) is the amount of biosorption at time  $t$  (min).

If second-order kinetics is applicable, the plot of  $t/q_t$  against  $t$  gives a straight line and  $q_e$  and  $k_2$  can be obtained from the slope and intercept of the plot, respectively. For investigated initial dye concentrations,  $k_2$  and corresponding correlation coefficients are presented in Table 1. The correlation coefficients were nearly equal to unity. The results indicated that the PSO biosorption mechanism is predominant for the biosorption of AB25 onto RS, and it is considered that the rate of the dye biosorption process is controlled by the chemisorption process.

5.3. Intraparticle Diffusion Models

To predict the rate controlling step of the AB25 biosorption, intraparticle diffusion model has been used. In general, any sorption process involves three main successive transport steps which are (i) film diffusion, (ii) intraparticle or pore diffusion, and (iii) sorption onto interior sites. The last step is considered negligible since it occurs rapidly, and hence, sorption should be controlled by either film diffusion or pore diffusion depending on which step is slower. The intraparticle diffusion model equation is expressed as:

$$q_t = k_{pi} t^{0.5} + C_i \tag{10}$$

Where,  $q_t$  (mg/g) is the amount of sorption at time  $t$  (min) and  $K_{pi}$  (mg/g.min<sup>-0.5</sup>) is the rate constant of intraparticle diffusion model. The intraparticle mass transfer curves at various AB25 concentrations. It

Table 1: PFO and PSO kinetic model

$C_0$ (mg/l)	$q_{e \text{ exp}}$ (mg/g)	model		PSO model	
		$k_1$ (1/min)	$R^2$	$k_2$ (1/min)	$R^2$
25	12.0391	0.0286	0.8725	0.0415	0.9978
50	21.1406	0.0811	0.9476	0.0627	0.9998
75	26.2969	0.0451	0.6338	0.0286	0.9995
100	34.8438	0.0504	0.9978	0.0107	0.9998

PFO: Pseudo-first-order, PSO: Pseudo-second-order

**Table 2:** Intraparticle diffusion models

Linear portion ↓	Constants ↓	C <sub>0</sub> =25 (mg/l)	C <sub>0</sub> =50 (mg/l)	C <sub>0</sub> =75 (mg/l)	C <sub>0</sub> =100 (mg/l)
First	K <sub>p1</sub> (mg/g.min <sup>-0.5</sup> )	0.6077	0.6367	1.9282	1.0382
	C <sub>1</sub> (mg/g)	8.3143	17.861	17.01	28.188
	R <sup>2</sup>	0.9589	0.9967	0.9967	0.9887
Second	K <sub>p2</sub> (mg/g.min <sup>-0.5</sup> )	0.3000	0.2754	0.3235	0.5814
	C <sub>2</sub> (mg/g)	0.9540	19.462	23.614	30.369
	R <sup>2</sup>	0.8424	0.9226	0.827	0.9899

was observed that the AB25 biosorption process trends to be followed by two distinct phases. The first phase is attributed to the diffusion of AB25 through the solution to the external surface of RS, and the second phase indicates the intraparticle diffusion of AB25 into the pores of RS. The intraparticle rate constants for the first step ( $k_{ip1}$ ), for the second phase ( $k_{ip2}$ ), and  $c$  parameters were obtained from the plot of  $q_t$  versus  $t^{0.5}$  and the results are given in Table 2. The values  $k_{id1}$  are higher than  $k_{ip2}$ , so it can be concluded that the rate-limiting step in present biosorption process is intraparticle diffusion. However, the lines did not pass through the origin (the plots have intercepts in the AB25 concentrations range of 25–100 mg/l) indicating that the intraparticle diffusion model is not the only rate-limiting mechanism. Therefore, it can be concluded that AB25 biosorption onto RS is a complex process and both intraparticle diffusion and surface sorption contribute to the rate-limiting step.

## 6. CONCLUSION

The RS was found to be one of the most promising biosorbents for the uptake of dyes due to its low cost, easy availability, and high dye uptake capacity. The utilization of RS may be the main advantage of the present study because it is an agricultural waste material. The AB25 removal efficiency of the RS was tested through dose, pH, kinetics, and equilibrium parameters. The biosorption pattern of AB25 onto RS was well fitted with PSO, biosorption mechanism is predominant, and dye biosorption process is controlled by the chemisorption process. The monolayer biosorption capacity of RS was found to be 35.58 mg/g using Langmuir model equations. The experimental results indicated that the RS can be successfully used for the removal of AB25 from aqueous solutions.

## 7. ACKNOWLEDGMENTS

The author L. Sivarama Krishna is grateful to the Graduate School and The Thailand Research Fund (IRG578001), Chulalongkorn University for providing financial support, Postdoctoral Fellowship under Rachadapisaek Sompote Fund. The author Mohammad Alamgir Kabir is grateful to the Government of the Peoples' Republic of Bangladesh for the financial assistance through the STREC project (Strengthening the Research and Exploration Capabilities of the Geological Survey of Bangladesh). The authors also express their deepest gratitude to the authorities of the University Kebangsaan Malaysia to organize this program.

## 8. REFERENCES

1. L. K. Sivarama, A. A. Sreenath, W. Y. W. Zuhairi, M. R. Taha, A. R. Varada, (2014) Indian jujuba seed powder as an eco-friendly and a low-cost biosorbent for removal of acid blue 25 from aqueous solution, *The Scientific World Journal*, **2014**: 1-11.
2. M. C. S. Reddy, L. Sivaramakrishna, A. V. Reddy, (2012) The use

of an agricultural waste material, *Jujuba* seeds for the removal of anionic dye (Congo red) from aqueous medium, *Journal of Hazardous Materials*, **203-204**: 118-27.

3. J. S. Cao, J. X. Lin, F. Fang, M. T. Zhang, Z.R. Hu, (2014) A new adsorbent by modifying walnut shell for the removal of anionic dye: Kinetic and thermodynamic studies, *Bioresource Technology*, **163**: 199-205.
4. J. Z. Guo, B. Li, L. Liu, K. Lv, (2014) Removal of methylene blue from aqueous solutions by chemically modified bamboo, *Chemosphere*, **111**: 225-231.
5. W. Zhang, H. Li, X. Kan, L. Dong, H. Yan, Z. Jiang, H. Yang, A. Li, and R. Cheng, (2012) Adsorption of anionic dyes from aqueous solutions using chemically modified straw, *Bioresource Technology*, **117**: 40-47.
6. C. Xia, Y. Jing, Y. Jia, D. Yue, J. Ma, X. Yin, (2011) Adsorption properties of congo red from aqueous solution on modi fi ed hectorite : Kinetic and thermodynamic studies, *Desalination*, **265**: 1-3, 81-87.
7. L. Sivaramakrishna, M. S. Reddy, M. Jagadeesh, W. Y. W. Zuhairi, M. R. Taha, A. V. Reddy, (2014) Evaluation of biomass, Indian *Jujuba* seed (IJS) for removal of congo red, *American Journal of Environmental Sciences*, **10**: 374-382.
8. G. Crini, (2006) Non-conventional low-cost adsorbents for dye removal: A review, *Bioresource Technology*, **97**: 1061-1085.
9. M. A. M. Salleh, D. K. Mahmoud, W. A. W. A. Karim, A. Idris, (2011) Cationic and anionic dye adsorption by agricultural solid wastes: A comprehensive review, *Desalination*, **280**: 1-13.
10. C. T. Weber, E. L. Foletto, L. Meili, (2013) Removal of tannery dye from aqueous solution using papaya seed as an efficient natural biosorbent, *Water, Air, and Soil Pollution*, **224**: 1427.
11. S. K. Ponnusamy, R. Subramaniam, (2013) Process optimization studies of Congo red dye adsorption onto cashew nut shell using response surface methodology, *International Journal of Industrial Chemistry*, **4**: 17.
12. V. K. Gupta, D. Pathania, S. Agarwal, S. Sharma, (2014) Amputation of congo red dye from waste water using microwave induced grafted *Luffa cylindrica* cellulosic fiber, *Carbohydrate Polymers*, **111**: 556-566.
13. N. A. Oladoja, I. A. Ololade, J. A. Idighe, E. E. Egbon, (2009) Equilibrium isotherm analysis of the sorption of congo red by palm kernel coat, *Central European Journal of Chemistry*, **7**: 760-768.
14. S. A. Tunali, Y. Y. Balk, O. Tuna, T. Akar, (2013) Improved biosorption potential of Thuja orientalis cone powder for the biosorptive removal of Basic Blue 9, *Carbohydrate Polymers*, **94**: 400-408.
15. R. Zhang, J. Zhang, X. Zhang, C. Dou, R. Han, (2014) Adsorption of congo red from aqueous solutions using cationic surfactant



- modified wheat straw in batch mode : Kinetic and equilibrium study, *Journal of the Taiwan Institute of Chemical Engineers*, **45**: 2578-2583.
16. L. K. Sivarama, A. R. Sreenath, A. Muralikrishna, W. Y. Z. Wan, H. Osman, A. R. Varada, (2015) Utilization of the agricultural waste (*Cicer arietinum* Linn fruit shell biomass) as biosorbent for decolorization of Congo red, *Desalination and Water Treatment*, **56**: 2181-2192.
  17. K. S. Bharathi, S. T. Ramesh, (2013) Removal of dyes using agricultural waste as low-cost adsorbents: A review, *Applied Water Science*, **3**: 773-790.
  18. Z. L. Yaneva, N. V. Georgieva, (2012) Insights into congo red adsorption on agro-industrial materials-spectral, equilibrium, kinetic, thermodynamic, dynamic and desorption studies. A review, *International Review of Chemical Engineering*, **4**: 127-146.
  19. V. Ponnusami, V. Gunasekar, S. N. Srivastava, (2009) Kinetics of methylene blue removal from aqueous solution using gulmohar (*Delonix regia*) plant leaf powder: Multivariate regression analysis, *Journal of Hazardous Materials*, **169**: 119-127.
  20. V. Ponnusami, S. Vikram, S. N. Srivastava, (2008) Guava (*Psidium guajava*) leaf powder: Novel adsorbent for removal of methylene blue from aqueous solutions, *Journal of Hazardous Materials*, **152**: 276-286.
  21. P. K. Senthil, S. Ramalingam, C. Senthamarai, M. Niranjanaa, P. Vijayalakshmi, S. Sivanesan, (2010) Adsorption of dye from aqueous solution by cashew nut shell: Studies on equilibrium isotherm, kinetics and thermodynamics of interactions, *Desalination*, **261**: 52-60.
  22. H. B. Senturk, D. Ozdes, C. Duran, (2010) Biosorption of Rhodamine 6G from aqueous solutions onto almond shell (*Prunus dulcis*) as a low cost biosorbent, *Desalination*, **252**: 81-87.
  23. L. D. T. Prola, E. Acayanka, E. C. Lima, C. Bestetti, W. O. Santos, F. A. Pavan, S. L. P. Dias, C. R. T. Tarley, (2013) Application of aqai stalks as biosorbent for the removal of Evans Blue and Vilmafix Red RR-2B dyes from aqueous solutions, *Desalination and Water Treatment*, **51**: 4582-4592.
  24. M. K. Dahri, L. B. L. Lim, N. Priyantha, C. M. Chan, (2016) Removal of acid blue 25 using cempedak durian peel from aqueous medium: Isotherm, kinetics and thermodynamics studies, *International Food Research Journal*, **23**: 1154-1163.
  25. N. Atar, A. Olgun, (2007) Removal of acid blue 062 on aqueous solution using calcinated colemanite ore waste, *Journal of Hazardous Materials*, **146**: 171-179.
  26. H. Aydın, G. Baysal, (2006) Adsorption of acid dyes in aqueous solutions by shells of bittim (*Pistacia khinjuk* Stocks), *Desalination*, **196**: 248-259.
  27. K. Badii, F. D. Ardejani, M. A. Saberi, N. Y. Limaee, (2010) Adsorption of acid blue 25 dye on diatomite in aqueous solutions, *Indian Journal of Chemical Technology*, **17**: 7-16.
  28. V. Jaikumar, K. S. Kumar, D. G. Prakash, (2009) Biosorption of acid dyes using spent brewery grains: Characterization and modeling, *International Journal of Applied Science and Engineering*, **7**: 115-125.
  29. M. Auta, B. H. Hameed, (2011) Preparation of waste tea activated carbon using potassium acetate as an activating agent for adsorption of Acid Blue 25 dye, *Chemical Engineering Journal*, **171**: 502-509.
  30. Z. X. Han, Z. Zhu, D. D. Wu, J. Wu, Y. R. Liu, (2014) Adsorption kinetics and thermodynamics of acid blue 25 and methylene blue dye solutions on natural sepiolite, *Synthesis and Reactivity in Inorganic Metal-Organic and Nano-Metal Chemistry*, **44**: 140-147.